Emodin treatment of papillary thyroid cancer cell lines *in vitro* inhibits proliferation and enhances apoptosis via downregulation of NF-κB and its upstream TLR4 signaling

XIN LIU[1,2*], WEI WEI[3*], YUE-ZHANG WU[2], YUAN WANG[2,4], WEI-WEI ZHANG[2,4], YONG-PING WANG[1], XIAO-PING DONG[2] and QI SHI[2]

[1]Basic Medical College, Guizhou University of Traditional Chinese Medicine, Guiyang, Guizhou 550025; [2]National Key-Laboratory of Intelligent Tracing and Forecasting for Infectious Disease, National Institute for Viral Disease Control and Prevention, Chinese Center for Disease Control and Prevention, Beijing 102206; [3]Key Laboratory of Carcinogenesis and Translational Research (Ministry of Education), Department of Head and Neck Surgery, Peking University Cancer Hospital and Institute, Beijing 100142; [4]Basic Medical College, North China University of Science and Technology, Tangshan, Hebei 063210, P.R. China

Received January 17, 2023; Accepted August 15, 2023

DOI: 10.3892/ol.2023.14101

Abstract. Thyroid cancer is one of the most common types of endocrine malignancy. In addition to surgical treatment, it is very important to find new treatment methods. The aim of the present study was to evaluate the effect of 1,3,8-trihydroxy-6-methylanthraquinone (emodin) on cellular NF-κB components and the upstream regulatory pathway of toll-like receptor 4 (TLR4) signaling, as well as the invasion and migration of papillary thyroid carcinoma (PTC) cells. The protein expression of NF-κB components p65 and p50 and their phosphorylated (p-) forms in the sections of PTC tissues was measured by individual immunohistochemical assays. PTC cell lines TPC-1 and IHH4 were exposed to 20 and 40 μM emodin for 24 h. The levels of the NF-κB components p65, p50, c-Rel, p-p65 and p-p50, elements in TLR4 signaling, including TLR4, MYD88 innate immune signal transduction adaptor (MyD88), interferon regulatory factor 3, AKT and MEK, and proliferative and apoptotic biomarkers, including c-Myc, cyclin D1, proliferating cell nuclear antigen, Bcl-2 and Bax, were evaluated by western blotting and immunofluorescent assays. The invasion and migration of PTC cell lines exposed to emodin were tested by plate colony and wound healing assay. Compared with hyperplasia tissue, the expression levels of NF-κB components p65 and p50, and p-p65 and p-p50 in PTC tissue were significantly increased. Treatment of PTC cell lines with emodin lead to significantly reduced levels of the aforementioned NF-κB components, accompanied by markedly downregulated TLR4 signaling. MYD 88-dependent and -independent pathways, are also significantly down-regulated. Downregulation of proliferative factors and activation of apoptotic factors were observed in the cell lines following treatment with emodin. Consequently, inhibition of the invasion and migration activities were observed in the emodin-treated PTC cells. Emodin could inhibit proliferation and promote apoptosis of PTC cells, which is dependent on the downregulation of cellular NF-κB and the TLR4 signaling pathway.

Correspondence to: Professor Qi Shi or Professor Xiao-Ping Dong, National Key-Laboratory of Intelligent Tracing and Forecasting for Infectious Disease, National Institute for Viral Disease Control and Prevention, Chinese Center for Disease Control and Prevention, 155 Chang-Bai Road, Beijing 102206, P.R. China
E-mail: shiqi@ivdc.chinacdc.cn
E-mail: dongxp238@sina.com

*Contributed equally

Key words: emodin, papillary thyroid cancer, NF-κB, toll-like receptor 4 signaling, proliferation

Introduction

Thyroid cancer is one of the most common types of endocrine malignancies (1). There are ≤43 types of thyroid cancer according to the new World Health Organization classification of thyroid tumors (2). Of these, differentiated thyroid cancer and papillary thyroid carcinoma (PTC) are the most frequent, accounting for ~80% of all thyroid cancer. PTC usually has a good clinical prognosis, with >90% of patients exhibiting a disease-specific survival of >10 years (3,4). However, histologically, interstitial TC may develop into thyroid-like carcinoma, which is a biological process that can induce a transition from a more differentiated state to a poorly differentiated state (5). Therefore, it is important to develop treatments for TC besides surgical operation.

1,3,8-trihydroxy-6-methylanthraquinone (emodin), with the chemical formula $C_{15}H_{10}O_5$, is primarily obtained from the *Polygonaceae* family and is the main active ingredient in Chinese herbal medicines rhubarb and *Polygonum cuspidatum* (6). Emodin has multiple biological activities, such as antibacterial, antitumor and hepatoprotective effects (7). It exhibits inhibitory effects on numerous types of malignant tumor, including liver, stomach, breast and pancreatic cancer (8-11). Studies have proposed that the antitumor effect of emodin is associated with its anti-NF-κB activity (12,13).

In the present study, the effects of emodin on levels of NF-κB components, upstream and downstream agents of NF-κB and the *in vitro* carcinoma features of two thyroid cancer cell lines were analyzed. The present study aimed to explore the mechanism of emodin in treatment of PTC and to provide theoretical support for the therapeutic effect of emodin on PTC.

Materials and methods

Ethics statement. Written informed consent regarding participation in the present study was obtained from patients. Samples were collected from 12 human samples used in this experiment. The age range was from 31 to 64; There were 5 male patients and 7 female patients. All samples were determined and collected in Peking University Cancer Hospital (Beijing, China) from January 2020 to January 2022. Use of stored human samples was approved by the Ethics Committees of Peking University Cancer Hospital and the Institute and National Institute for Viral Disease Prevention and Control, China CDC (approval no. IVDC2021-12, Beijing, China).

Reagents and antibodies. Emodin and dimethyl sulfoxide were purchased from MilliporeSigma. The antibodies included antibodies for p65 (cat. no. sc-8008), phosphorylated (p-)p65 (cat. no. sc-136548), p50 (cat. no. sc-114), p-p50 (cat. no. sc-271908), c-Rel (cat. no. sc-6955), cyclin D1 (cat. no. sc-8396), c-Myc (cat. no. sc-40), PCNA (cat. no. sc-56), TLR4 (cat. no. sc-293072), IRF3 (cat. no. sc-33641), AKT1/2/3 (cat. no. sc-56878), MEK1/2 (cat. no. sc-81504), Bcl-2 (cat. no. sc-7382), Bax (cat. no. sc-7480). The above antibodies are from Santa Cruz Biotechnology, Inc., WB dilution concentration is 1:200, IHC and IFA dilution concentration is 1:50. MyD88 (cat. no. ab113739; Abcam, WB dilution concentration is 1:2,000; IFA dilution concentration is 1:200) and β-actin (cat. no. AB0145-200; OriGene Technologies; 1:5,000), HRP-AffiniPure Goat Anti-Rabbit IgG (H+L) Secondary (cat. no. 111-035-003; Jackson ImmunoResearch Laboratories, Inc.), HRP-AffiniPure Goat Anti-Mouse IgG (H+L) Secondary (cat. no. 115-035-003; Jackson ImmunoResearch Laboratories, Inc.).

Cell culture. PTC cell lines TPC-1 and IHH4 were used (14-16). TPC-1 and IHH4 cell lines were purchased from Zhejiang Meisen Cell Technology Co., Ltd. Cells were identified by short tandem repeat analysis and did not exhibit contamination or infection with mycoplasma, bacteria or fungi. Cells were cultured in DMEM (cat. no. 11965118; Thermo Fisher Scientific Inc.) containing 10% fetal bovine serum (cat. no. 10270106; Thermo Fisher Scientific Inc.) and 1% penicillin-streptomycin (cat. no. 15140122; all Thermo Fisher Scientific Inc.) in an incubator at 37˚C with 5% CO_2. Emodin was dissolved in buffer containing 0.1% DMSO. The cells in treatment groups were separately exposed to 20 and 40 μM emodin; cells in the mock group were exposed to buffer containing only 0.1% DMSO. Cells were exposed to treatment at 37˚C for 24 h. Considering that DMSO at ≤0.1% has no significant effect in cell activity-related experiments (17), a blank cell control was not included.

Cell viability assay. Cell viability was assessed using a Cell Counting Kit-8 (CCK-8; cat. no. CK04; Dojindo Molecular Laboratories, Inc.) according to manufacturer's instructions. Briefly, after cells were cultured with emodin (10, 20, 40, 60, 80 or 100 μM) at 37˚C for 24 h, 10 μl CCK-8 was added to each well at 37˚C and 5% CO_2 for 1 h. The optical density (OD) at 450 nm was measured using a microplate reader (Thermo Fisher Scientific, Inc.). Relative cell viability was calculated by comparing OD_{450} of the experimental group to that of the control group. The cell survival rate was calculated as follows: Cell survival rate (%)=(Experimental OD-blank OD)/(control OD-blank OD) x100%.

Immunohistochemistry (IHC). Surgically removed tumor tissues were fixed in 10% buffered formalin solution at 4˚C for 12 h and paraffin sections of thickness of 2 μm were routinely prepared. The paraffin sections of PTC tissue were dewaxed and dehydrated with xylene and alcohol and repaired using a microwave at 100˚C for 30 min. Samples were blocked with 3% hydrogen peroxide (cat. no. AR1108; Wuhan Boster Biological Technology, Ltd.) at room temperature (RT) for 10 min. After blocking with 10% normal goat serum (cat. no. AR1009; Wuhan Boster Biological Technology, Ltd.) at room temperature (RT) for 15 min, sections were incubated with primary antibodies (p65: cat. no. sc-8008; p-p65: cat. no. sc-136548; p50: cat. no. sc-114; p-p50: cat. no. sc-271908) at 4˚C overnight, and secondary antibodies (Enzyme-labeled goat anti-mouse IgG polymer: PV-6002, Enzyme-labeled goat anti-rabbit IgG polymer: PV-6002; Beijing Zhong Shan Goldenbridge Biotechnology Company Ltd.) at 37˚C for 40 min. For visualization, slices were incubated with 3,3-diaminobenzidine tetrahydrochloride (cat. no. AR1000; Wuhan Boster Biological Technology, Ltd.) at RT for 3 min, counterstained with hematoxylin (cat. no. AR 0005; Wuhan Boster Biological Technology, Ltd.) at RT for 1 min, dehydrated and seal the sample with resin and cover glass (cat. no. 10212450C; Citotest Scientific Co., Ltd.). Then use a light microscope to enlarge it by 400 times. Analysis was performed using ImageJ (version 1.8.0; National Institutes of Health) measurement results.

Western blotting. After washing cells with PBS three times, cultured cells were collected and harvested by centrifugation at 37˚C at 500 x g for 10 min. Resulting pellets were lysed at 4˚C for 1 h using Mammalian Protein Extraction kit (cat. no. CW0889; CoWin Biosciences) with protease inhibitor Cocktail set III (1%; v/v; cat. no. 535140; Merck KGaA), followed by centrifugation at 4˚C at 500 x g for 10 min and supernatants were collected. Protein concentration was estimated using a BCA protein assay kit (cat. no. 71285-3; Merck KGaA). Cell lysates (70-100 μg/lane) were separated by 12% SDS-PAGE and electroblotted onto nylon membranes. The membranes were blocked with Tris-buffered saline (pH 7.6) containing 0.05% Tween-20 and 5% skimmed milk at RT for 1 h, then incubated with antibodies [p65 (cat. no. sc-8008); p-p65 (cat. no. sc-136548); p50 (cat. no. sc-114); p-p50 (cat. no. sc-271908); c-Rel (cat. no. sc-6955); cyclin D1 (cat. no. sc-8396); c-Myc (cat. no. sc-40); PCNA (at. no. sc-56); TLR4 (cat. no. sc-293072); IRF3 (cat. no. sc-33641); AKT1/2/3 (at. no. sc-56878); MEK1/2 (cat. no. sc-81504); Bcl-2 (cat. no. sc-7382); Bax (cat. no. sc-7480). The above antibodies are from Santa Cruz Biotechnology, Inc., WB dilution concentration is 1:200. MyD88 (cat. no. ab113739; Abcam; WB dilution concentration is 1:2,000) and β-actin (cat. no. AB0145-200; OriGene Technologies, Inc.; 1:5,000)] overnight at 4˚C. The

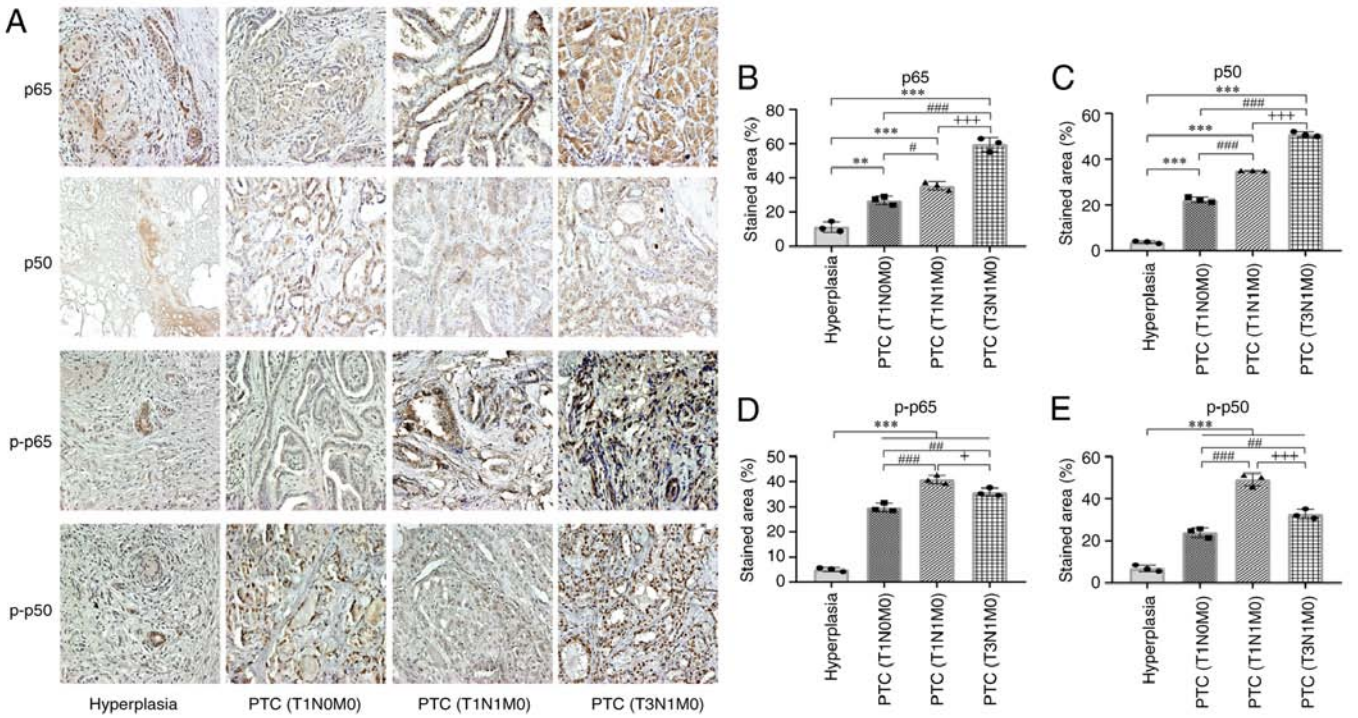

Figure 1. Expression of NF-κB components p65, p50, p-p65 and p-p50 in the tissues of PTC and benign hyperplasia in immunohistochemical assays. (A) Immunohistochemical assays for p65, p50, p-p65 and p-p50. (B) Quantification of p65. (C) Quantification of p50. (D) Quantification of p-p65. (E) Quantification of p-p50. The representative images are shown; magnification, x400. **P<0.01 and ***P<0.001 vs. Hyperplasia; $^{\#\#}$P<0.01 and $^{\#\#\#}$P<0.001 vs. PTC (T1N0M0); $^{+}$P<0.01 and $^{+++}$P<0.001 vs. PTC (T1N1M0). TNM, tumor-node-metastasis; PTC, papillary thyroid carcinoma; p, phosphorylated.

membranes were incubated with secondary antibodies [rabbit secondary antibody (cat. no. 111-035-003); mouse secondary antibody (cat. no. 115-035-003); The above antibodies are from Jackson ImmunoResearch Laboratories, Inc., WB dilution concentration is 1:5,000] at RT for 1 h. The blots were developed using Western Lightning Plus-ECL (cat. no. NEL105001EA; PerkinElmer, Inc.). Semi-quantitative analysis was performed using a Clinx ChemiCapture System with ChemiScope 6000 (Clinx Science Instruments Co., Ltd.). Using ImageJ (version 1.8.0; National Institutes of Health) measures gray values.

Immunofluorescence assay (IFA). Firstly, 0.4% paraformaldehyde was used to fix cells at RT for 20 min. Following treatment with 0.3% Triton-X100 at RT for 30 min and blocking with 5% BSA for 1 h at RT, cells were incubated with antibodies [p65 (cat. no. sc-8008); p-p65 (cat. no. sc-136548); p50 (cat. no. sc-114); p-p50 (cat. no. sc-271908); c-Rel (cat. no. sc-6955); cyclin D1 (cat. no. sc-8396); c-Myc (cat. no. sc-40); PCNA (cat. no. sc-56); TLR4 (cat. no. sc-293072); IRF3 (cat. no. sc-33641); AKT1/2/3 (cat. no. sc-56878); MEK1/2 (cat. no. sc-81504); Bcl-2 (cat. no. sc-7382); Bax (cat. no. sc-7480). The above antibodies are from Santa Cruz Biotechnology, Inc., IFA concentration is 1:50. MyD88 (cat. no. ab113739; Abcam; 1: 200)] at 4˚C overnight. Cells were incubated with secondary antibodies (1:200; Alexa Fluor 488 anti-rabbit or Alexa Fluor 568 anti-mouse; cat. nos. A32731 and A32723, respectively; both Thermo Fisher Scientific, Inc.) at 37˚C for 1 h. Following counterstaining with 1 μg/ml DAPI (Beyotime Institute of Biotechnology) at RT for 20 min, images were captured using a Leica TCS SP8 confocal microscope (Leica Microsystems, Ltd.).

Colony formation assay. Cells were digested with trypsin, a total of 1,000 cells/well was seeded in six-well plates and incubated at 37˚C for 12 h. Cells were treated with different concentrations of emodin (20, 40 μM) at 37˚C for 7 days. Next, 0.4% paraformaldehyde was used to fix cells at RT for 20 min. And stained with crystal violet at RT for 3 min and images were taken under a light microscope (magnification, x40 times. When there are more than 50 cells, it can be judged as a colony. Using ImageJ (version 1.8.0; National Institutes of Health), colonies were counted (18).

Wound healing assay. Wound healing assay was performed to evaluate cell migration. Cells were seeded in a six-well plate and grew to confluence rate of 100%, followed by scratching the monolayer with a 200-μl pipette tip to create a wound. Plates were washed to remove floating cells and debris, DMEM containing 1% fetal bovine serum was added. Then treated with emodin (20, 40 μM) at 37˚C for 24 h. The cell migration images were captured at 0 and 24 h post-treatment using a light microscope (magnification, x40). Each group contained ≥3 independent wells.

Statistical analysis. Statistical analysis was performed using SPSS (version 22.0; IBM Corp.). Quantification of IFA as integrated option density) was performed using ImageJ (version 1.8.0; National Institutes of Health). All experiments were conducted ≥3 times. All data are presented as the mean ± SD. Difference among cells treated with different concentrations of emodin and mock cells in CCK-8 was determined using unpaired t test. Significant differences between cells treated with different concentrations of emodin and mock cells in western blotting, IHC, IFA, colony formation and wound

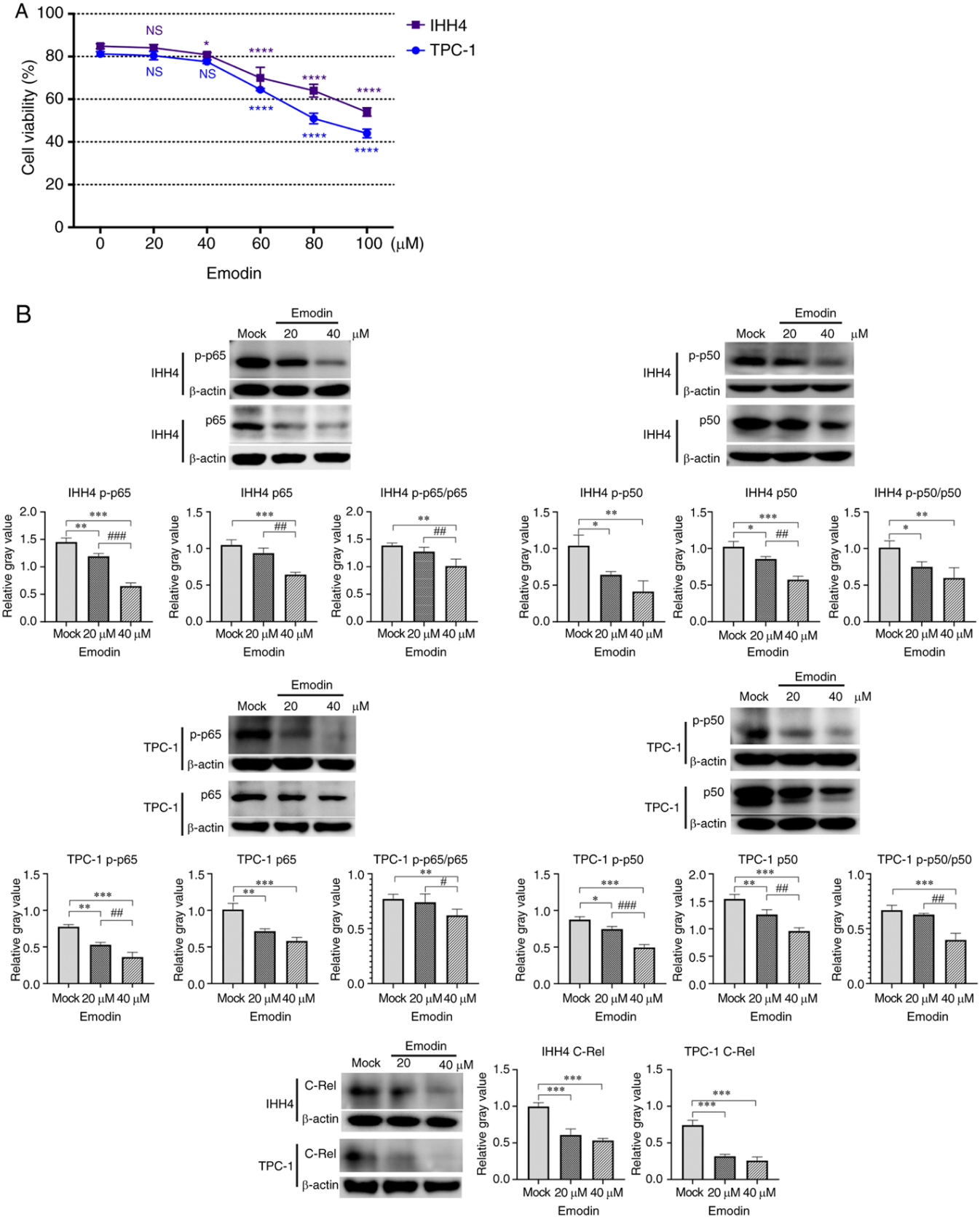

Figure 2. Continued.

healing assay were determined using one-way ANOVA followed by Tukey's post hoc test. P<0.05 was considered to indicate a statistically significant difference.

Results

PTC tissue expresses higher levels of NF-κB components

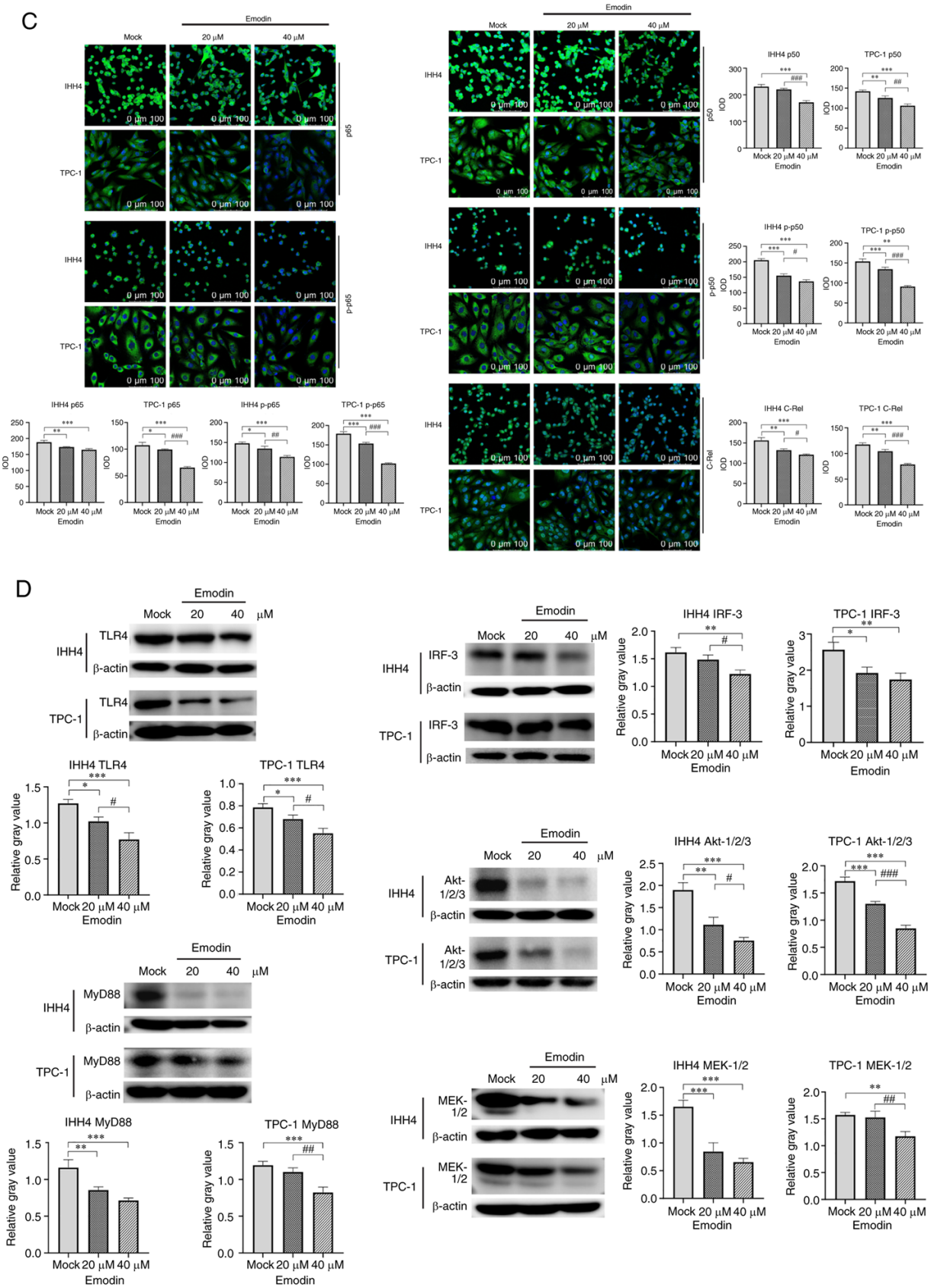

Figure 2. Continued.

p65 and p50, as well as p-p65 and p-p50. An increase in NF-κB activity has been described in numerous types of malignant tumor (19). Tissue sections of PTC at different stages, including three tumor (T)1 node (N)0 metastasis (M)0, three T1N1M0 and three T3N1M0, as well as three benign hyperplastic tissues, were subjected to IHC with antibodies for

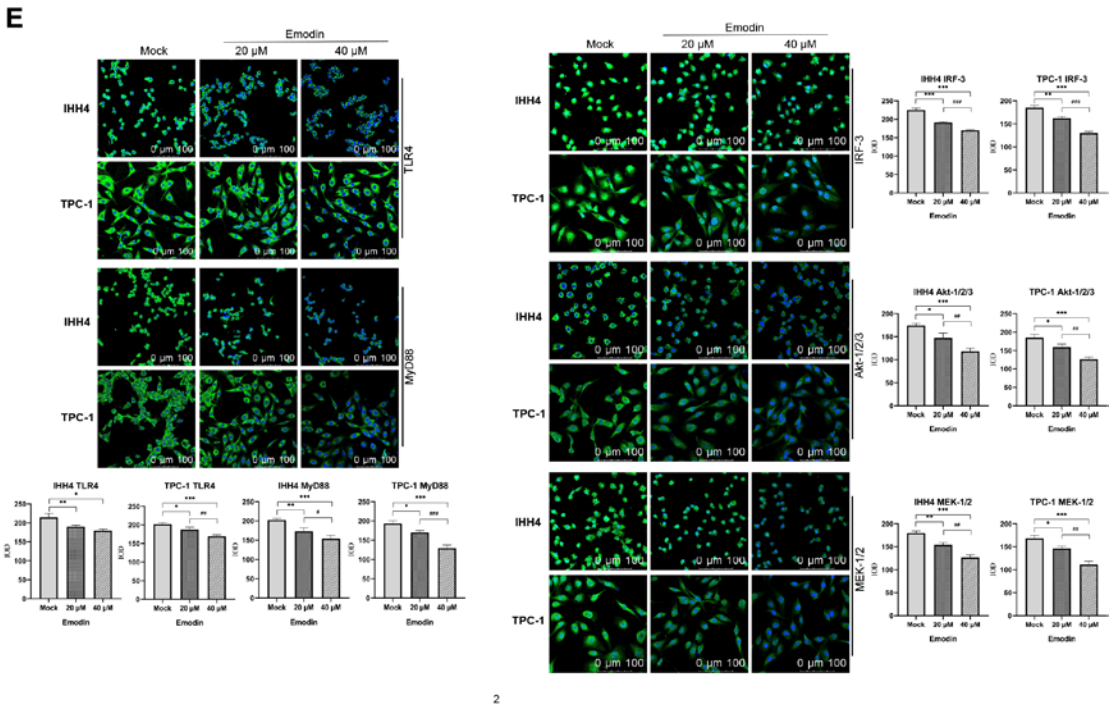

Figure 2. Expression of NF-κB components TLR4, MyD88, IRF3, AKT and MEK decreases in thyroid cancer cell lines IHH4 and TPC-1 following treatment with emodin. (A) Cell Counting Kit-8 assays. TPC-1 and IHH4 cells were exposed to emodin dissolved in the buffer containing 0.1% DMSO. The data were normalized with that of blank control without emodin. Representative (B) western blots and (C) IFAs for p65, p50, p-p65, p-p50 and C-Rel. Representative (D) western blots and (E) IFAs for TLR4, MyD88, IRF3, AKT and MEK. *P<0.05, **P<0.01, ***P<0.001 and ****P<0.0001 vs. Mock; $^{\#}$P<0.05, $^{\#\#}$P<0.01 and $^{\#\#\#}$P<0.001 vs. 20 μM emodin). TLR4, toll-like receptor 4; IFA, immunofluorescence assay; p, phosphorylated; MyD88, MYD88 innate immune signal transduction adaptor; IRF3, interferon regulatory factor 3; IOD, integrated option density; emodin, 1,3,8-trihydroxy-6-methylanthraquinone; NS, not significant.

NF-κB components (Fig. 1A). Compared with benign thyroid hyperplasia tissue, more staining was observed in PTC tissue via IHC analysis of p65 and p50 (Fig. 1B and C), particularly in PTC T1N1M0 and T3N1M0. Quantitative assay of the signal intensity revealed increased levels of p65 and p50 in PTC tissue and the percentage of the positive area increased with progression of tumor stages. Subsequently, IHC of p-p65 and p-p50 demonstrated that more staining were detected in PTC tissues (Fig. 1D and E). Significantly higher percentages of positive areas of p65, p50, p-p65 and p-p50 were calculated for PTC compared with benign tissues in the quantitative assays.

Emodin treatment of thyroid cancer cell lines downregulates NF-κB via inhibition of the TLR4 signaling pathway. Prior to testing the effect of emodin on the NF-κB components and upstream TLR4 signaling, thyroid cancer cell lines IHH4 and TPC-1 were treated with various concentrations of emodin (10, 20, 40, 60, 80 or 100 μM) to assess cytotoxicity. Cells were harvested at 24 h post-exposure and subjected to CCK-8 assay. The data of the individual preparations were normalized with that of the cells without emodin, set as 100%. As emodin concentration increased, the survival rate of cells decreased. Compared with the preparations treated with DMSO not containing emodin (0 μM), the viability of the cells treated with 20 and 40 μM emodin was slightly decreased, while cells exposed to ≥60 μM emodin had significantly decreased viability (Fig. 2A). Based on the results of CCK-8 assays, 20 and 40 μM emodin were used in subsequent experiments. At 24 h after exposure, emodin-treated cells and the mock cells exposed to 0.1% DMSO buffer were harvested. Western blotting of cellular lysates revealed that the signals of NF-κB components p65, p50 and c-Rel, as well as p-p65 and p-p50, were significantly weaker in cells treated with emodin compared with the mock group, the ratio of p-p65 to p65, p-p50 to p50 were significantly decreased (Fig. 2B). IFA also revealed significantly weaker green staining in emodin-treated IHH4 and TPC-1 cells (Fig. 2C). The effect of 40 μM emodin on various NF-κB components was stronger than that of 20 μM.

The levels of elements in the upstream regulatory pathway for NF-κB, including TLR4, MyD88, IRF3, AKT and MEK, in IHH4 and TPC-1 cells were examined after exposure to emodin or DMSO. Western blotting demonstrated that expression of TLR4, MyD88, IRF3, AKT and MEK in the emodin-treated cells was significantly weaker than in the mock cells exposed to DMSO (Fig. 2D). IFA revealed that the fluorescence intensities of TLR4, MyD88, IRF3, AKT and MEK in the emodin-treated cells was significantly weaker than in the mock cells exposed to DMSO (Fig. 2E) in emodin-treated cells. This indicated that emodin treatment of thyroid cell lines inhibited the upstream regulatory TLR4 signaling pathway of NF-κB.

Emodin treatment of thyroid cancer cell lines suppresses proliferative factors and promotes apoptotic factors. To examine the effects of emodin on cellular levels of proteins involved in cell proliferation and apoptosis, thyroid cancer cell lines treated with or without emodin were subjected to western blotting and IFA. Compared with the control group, the protein expression levels of PCNA, cyclin D1 and c-Myc in the cells treated with emodin significantly decreased (Fig. 3A).

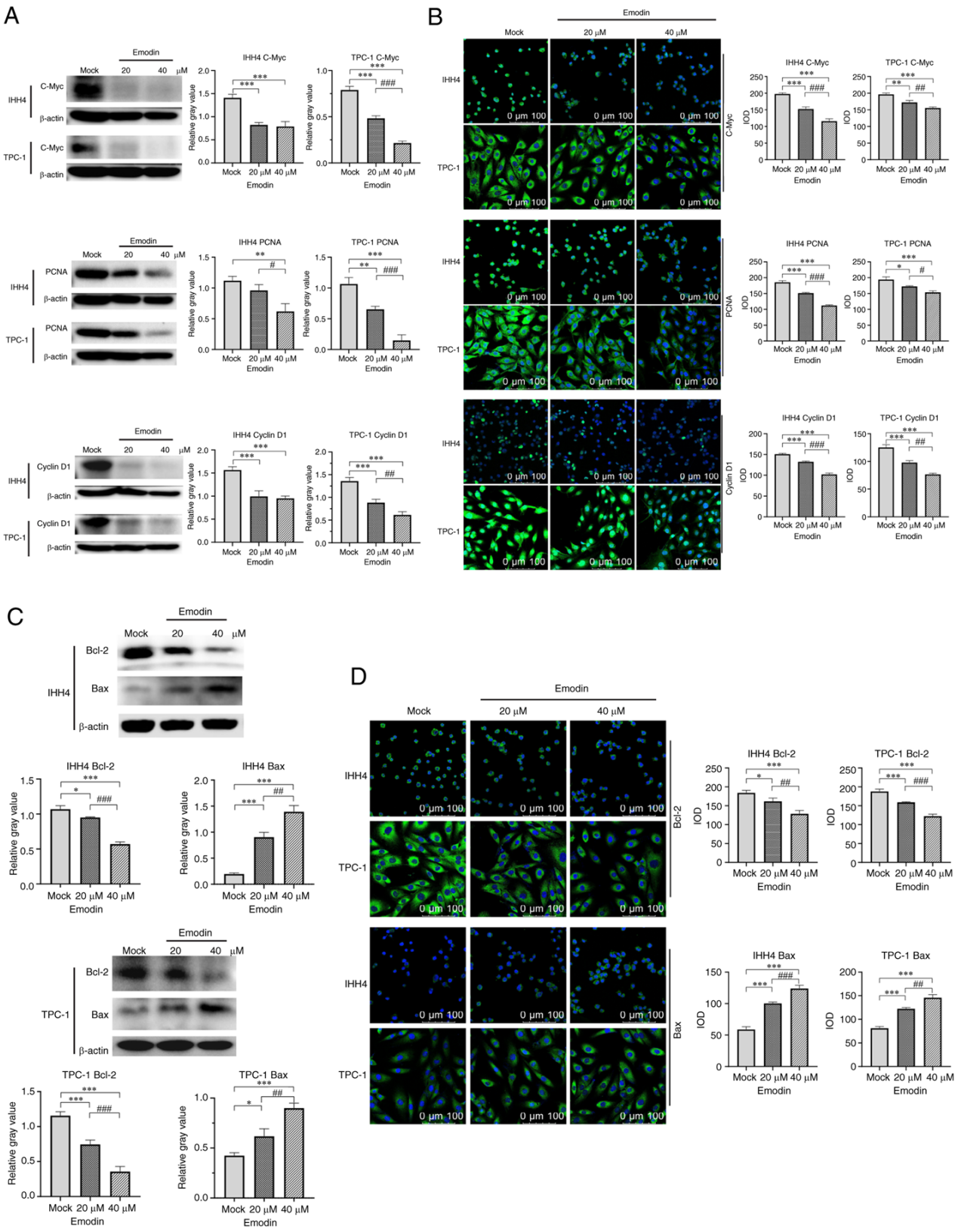

Figure 3. Changes of cell cycle and apoptotic proteins in IHH4 and TPC-1 cells following treatment with emodin. Representative (A) western blots and (B) IFAs for PCNA, cyclin D1 and c-myc. Representative (C) western blots and (D) IFAs for Bcl-2 and Bax. *P<0.05, **P<0.01 and ***P<0.001 vs. Mock; $^{\#}$P<0.05, $^{\#\#}$P<0.01 and $^{\#\#\#}$P<0.001 vs. 20 μM (emodin). Emodin, 1,3,8-trihydroxy-6-methylanthraquinone; PCNA, proliferating cell nuclear antigen; IFA, immunofluorescence assay; IOD, integrated option density.

Significantly lower fluorescence intensities in emodin-treated IHH4 and TPC-1 cells were also identified in PCNA, cyclin D1 and c-Myc (Fig. 3B). Furthermore, the levels of apoptotic Bcl-2 and Bax were examined. Both western blotting and IFA

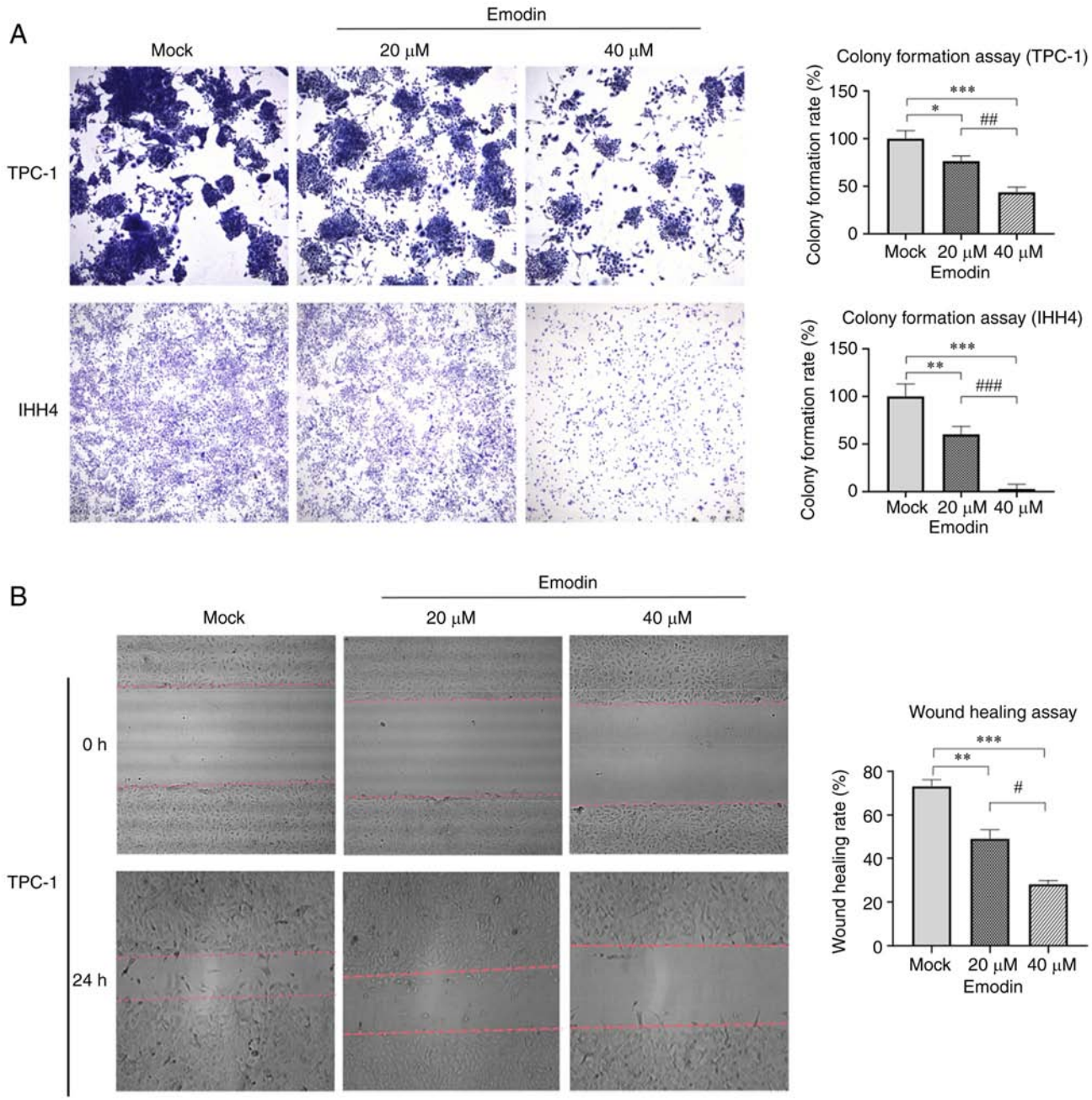

Figure 4. Carcinoma-associated characteristics of IHH4 and TPC-1 cells after treatment with emodin. Representative (A) colony formation and (B) wound healing assay. Magnification, x400; *P<0.05, **P<0.01 and ***P<0.001 vs. Mock. $^{\#}$P<0.05, $^{\#\#}$P<0.01 and $^{\#\#\#}$P<0.001 vs. 20 μM (emodin). Emodin, 1,3,8-trihydroxy-6-methylanthraquinone.

revealed a decrease and an increase in Bcl-2 and Bax levels, respectively, in the cells treated with emodin (Fig. 3C and D).

Emodin inhibits migration of thyroid cancer cell lines in vitro. To assess the influence of emodin on tumor characteristics such as proliferation, apoptosis, migration, and invasion of IHH4 and TPC-1 cells (20), cells were assessed using a colony formation assay after treatment with and without emodin for 7 days. A lower number and smaller size of colonies were observed in cells receiving 20 and 40 μM emodin compared with those in the mock cells (Fig. 4A). The wound healing assay showed that the number of TPC-1 cells treated with emodin for 24 h was lower than that of the control group (Fig. 4B). This demonstrated that exposure to emodin decreased colony formation and migration of thyroid cancer cells *in vitro*.

Discussion

Recent studies have demonstrated that emodin inhibits proliferation and promotes apoptosis of PTC cells by regulating the AMP-activated protein kinase signaling pathway and mediating VEGFR-2 expression (21,22). However, studies of the effect of emodin on inflammatory pathways in TC cells are relatively limited (21,23). As a core element of the inflammatory reaction, the NF-κB signaling pathway is involved in the pathophysiological processes of breast cancer, colon cancer, leukemia, lung cancer and other tumors (19). Serving as an

important transcription factor, NF-κB is widely distributed in lymphocytes, skeletal cells, mouse mammary epithelium, fibroblasts or human epithelial cells and other cells and controls cell stress and survival (24-26). Dysregulation of NF-κB is associated with malignant neoplasia, inflammation, viral infection and autoimmune disease (rheumatoid arthritis, insulin-dependent diabetes mellitus and multiple sclerosis) (27-29). In line with previous studies (29,30), aberrant upregulation of NF-κB components in thyroid cancer tissue was assessed in the present study. Using cultured PTC cell lines, the present study verified that emodin exposure can reverse the upregulation of NF-κB components such as p65, p50, p-p65, p-p50 and c-Rel, which may affect cell proliferation, apoptosis and carcinogenicity.

The present study revealed that levels of the NF-κB upstream components, including TLR4, MyD88, IRF3, AKT and MEK, were downregulated in the PTC cell lines following exposure to emodin. TLR4 is positively associated with the development of liver cancer, breast cancer, cervical cancer and other cancers, and has an immunosuppressive function and promotes survival of cancer cells (31,32). There are two primary pathways of TLR4 signaling: MyD88-dependent and -independent pathway. In the MyD88-dependent pathway, TLR4 combines with MyD88, forming an active TLR4/MyD88 complex. Through molecular interaction and phosphorylation, including recruiting IL-1 and binding to TNF receptor-associated factor 6, activating MEK and AKT, inducing depolymerization of inhibitory factors, cellular NF-κB is activated, resulting in phosphorylation of p65 and p50 (1,33-35). In the MyD88-independent pathway, TLR4 directly activates IRF3, which is associated with activation of NF-κB downstream (36). p-p65 and p-p50 can be transferred from the cytoplasm to the nucleus and, as transcription regulators, they participate in activation of the NF-κB pathway (34,37). c-Rel is an important member of the NF-κB family. It usually forms a heterodimer with p65 or p50 to participate in activation of NF-κB. Additionally, c-Rel can activate target genes such as Bcl-XL and enhancer of zeste 2 polycomb repressive complex 2 subunit to promote cell proliferation (38,39). Continuous activation of NF-κB is associated with formation, development and metastasis of gastric cancer, colorectal cancer, leukemia and other tumors (40-42). The present data indicated that emodin inhibited TLR4 signaling via both MyD88-dependent and -independent pathways, and thus it was hypothesized that the antitumor activity of emodin depends on the inhibition of NF-κB via downregulation of the TLR4 signaling pathway.

The present study revealed downregulation of proliferative factors, including c-Myc, cyclin D1 and PCNA, as well downregulation of anti-apoptotic Bcl-2, and upregulation of the pro-apoptotic factor Bax in PTC cell lines exposed to emodin. One of the key biological functions of NF-κB is to control and regulation of expression and activities of a series of cell cycle factors such as cyclins A, H and p21 (26). A number of cell cycle proteins are targets of NF-κB, including c-Myc, c-Rel, IRF4 and cyclins D1, D2 and D3. The anti-apoptotic Bcl-2 and Bax are also targets of NF-κB. Knockdown of TLR4 in cervical cancer cells markedly increases the apoptosis rate, while TLR4 upregulates Bcl-2 via the NF-κB signaling pathway and promotes the proliferation of cancer cells (43). Therefore, it was hypothesized that emodin-induced changes in cell cycle and apoptotic proteins are largely due to its inhibitory effect on NF-κB.

The preliminary *in vitro* data of the carcinoma-associated characteristics of PTC cell lines following treatment with emodin highlighted the potential use of emodin to reverse tumorgenicity of PTC. The therapeutic potential of emodin in different types of malignant tumors has been examined repeatedly (8-11). Although the majority of patients with PTC have a good prognosis, endocrine and radionuclide therapy are sometimes needed besides surgical operation (44,45). The present study provided molecular evidence of the antitumor potential of emodin.

Acknowledgements

Not applicable.

Funding

The present study was supported by National Key R&D Program of China (grant no. 2020YFE0205700), State Key Laboratory of Infectious Disease Development Grant (grant nos. 2019 SKLID501, 2019 SKLID307 and 2021SKLID101).

Availability of data and materials

The datasets used and/or analyzed during the current study are available from the corresponding author on reasonable request.

Authors' contributions

XL, YZW, YW, and WWZ performed CCK-8, western blot, IFA, colony formation and wound healing assay. WW collected samples and performed IHC. XL and YPW conducted statistical analysis. XPD and QS obtained financial support and designed the study. XL, YPW, XPD and QS wrote the manuscript. All authors have read and approved the final manuscript. LX and WYZ confirm the authenticity of all the raw data.

Ethics approval and consent to participate

Use of the stored surgical removed samples was approved by Research Ethics Committee of the National Institute for Viral Disease Control and Prevention (approval no. IVDC2021-12, Beijing, China). Patients provided written informed consent for use of clinical material.

Patient consent for publication

Not applicable.

Competing interests

The authors declare that they have no competing interests.

References

1. Siegel RL, Miller KD and Jemal A: Cancer statistics, 2019. CA Cancer J Clin 69: 7-34, 2019.

2. Lloyd RV, Osamura RY, Klöppel G and Rosai J: WHO classification of tumours of endocrine organs. 4th edition. IARC Publications, Lyon, 2017.
3. Saini S, Tulla K, Maker AV, Burman KD and Prabhakar BS: Therapeutic advances in anaplastic thyroid cancer: A current perspective. Mol Cancer 17: 154, 2018.
4. Fagin JA and Wells SA Jr: Biologic and clinical perspectives on thyroid cancer. N Engl J Med 375: 1054-1067, 2016.
5. Boumahdi S and de Sauvage FJ: The great escape: Tumour cell plasticity in resistance to targeted therapy. Nat Rev Drug Discov 19: 39-56, 2020.
6. Zeng P, Shi Y, Wang XM, Lin L, Du YJ, Tang N, Wang Q, Fang YY, Wang JZ, Zhou XW, *et al*: Emodin rescued hyperhomocysteinemia-induced dementia and Alzheimer's disease-like features in rats. Int J Neuropsychopharmacol 22: 57-70, 2019.
7. Wang X, Wang J, Shi X, Pan C, Liu H, Dong Y, Dong R, Mang J and Xu Z: Proteomic analyses identify a potential mechanism by which extracellular vesicles aggravate ischemic stroke. Life Sci 231: 116527, 2019.
8. Fu JM, Zhou J, Shi J, Xie JS, Huang L, Yip AY, Loo WT, Chow LW and Ng EL: Emodin affects ERCC1 expression in breast cancer cells. J Transl Med 10 (Suppl 1): S7, 2012.
9. Wang Y, Yu H, Zhang J, Ge X, Gao J, Zhang Y and Lou G: Anti-tumor effect of emodin on gynecological cancer cells. Cell Oncol (Dordr) 38: 353-363, 2015.
10. Zhou RS, Wang XW, Sun QF, Ye ZJ, Liu JW, Zhou DH and Tang Y: Anticancer effects of emodin on HepG2 cell: Evidence from bioinformatic analysis. Biomed Res Int 2019: 3065818, 2019.
11. Yang Q, Leong SA, Chan KP, Yuan XL and Ng TK: Complex effect of continuous curcumin exposure on human bone marrow-derived mesenchymal stem cell regenerative properties through matrix metalloproteinase regulation. Basic Clin Pharmacol Toxicol 128: 141-153, 2021.
12. Stompor-Gorący M: The health benefits of emodin, a natural anthraquinone derived from rhubarb-a summary update. Int J Mol Sci 22: 9522, 2021.
13. Zhang Q, Chen WW, Sun X, Qian D, Tang DD, Zhang LL, Li MY, Wang LY, Wu CJ and Peng W: The versatile emodin: A natural easily acquired anthraquinone possesses promising anticancer properties against a variety of cancers. Int J Biol Sci 18: 3498-3527, 2022.
14. Chen F, Li M and Zhu X: Propofol suppresses proliferation and migration of papillary thyroid cancer cells by down-regulation of lncRNA ANRIL. Exp Mol Pathol 107: 68-76, 2019.
15. Le F, Luo P, Ouyang Q and Zhong X: LncRNA WT1-AS downregulates survivin by upregulating miR-203 in papillary thyroid carcinoma. Cancer Manag Res 12: 443-449, 2020.
16. Wang N, Duan H, Zhang C, Zhou Y and Gao R: The LINC01186 suppresses cell proliferation and invasion ability in papillary thyroid carcinoma. Oncol Lett 16: 5639-5644, 2018.
17. Qiu XX, Sun J, Zhao M, Chu X, An J and Li W: Inhibitory effects of emodin on the biological activity of human papillary thyroid cancer cells and related mechanisms. Acta Acad Med Xuzhou 41: 367-372, 2021 (In Chinese).
18. Rajendran V and Jain MV: In vitro tumorigenic assay: Colony forming assay for cancer stem cells. Methods Mol Biol 1692: 89-95, 2018.
19. Pramanik KC, Makena MR, Bhowmick K and Pandey MK: Advancement of NF-κB signaling pathway: A novel target in pancreatic cancer. Int J Mol Sci 19: 3890, 2018.
20. Hanahan D and Weinberg RA: Hallmarks of cancer: The next generation. Cell 144: 646-674, 2011.
21. Li W, Wang D, Li M and Li B: Emodin inhibits the proliferation of papillary thyroid carcinoma by activating AMPK. Exp Ther Med 22: 1075, 2021.
22. Zhang W, Peng Y and Teng Y: Inhibitory effects of emodin alone and its combination with gemcitabine on human thyroid cancer cell K1. Chin J Tradit Med Sci Technol 28: 733-738, 2021 (In Chinese).
23. Shi GH and Zhou L: Emodin suppresses angiogenesis and metastasis in anaplastic thyroid cancer by affecting TRAF6-mediated pathways *in vivo* and *in vitro*. Mol Med Rep 18: 5191-5197, 2018.
24. Yamamoto Y and Gaynor RB: Role of the NF-kB pathway in the pathogenesis of human disease states. Curr Mol Med 1: 287-296, 2001.
25. Zinatizadeh MR, Schock B, Chalbatani GM, Zarandi PK, Jalali SA and Miri SR: The nuclear factor kappa B (NF-kB) signaling in cancer development and immune diseases. Genes Dis 8: 287-297, 2020.
26. Ledoux AC and Perkins ND: NF-κB and the cell cycle. Biochem Soc Trans 42: 76-81, 2014.
27. Bacher S and Schmitz ML: The NF-kappaB pathway as a potential target for autoimmune disease therapy. Curr Pharm Des 10: 2827-2837, 2004.
28. Geng Xue CW and Lin Xiaoyue: Mechanism of NF-κB signaling pathway regulating lung cancer and research progress in intervention of traditional Chinese medicine. Chin J Exp Tradit Med Formulae: 1-11, 2023.
29. Sun J X Yy and Li J H: Expression&clinical significance of NF-κB in papillary thyroid carcinoma(PTC). J Microbiol 35: 58-61, 2015.
30. Faria M, Matos P, Pereira T, Cabrera R, Cardoso BA, Bugalho MJ and Silva AL: RAC1b overexpression stimulates proliferation and NF-kB-mediated anti-apoptotic signaling in thyroid cancer cells. PLoS One 12: e0172689, 2017.
31. Liu Y, Li T, Xu Y, Xu E, Zhou M, Wang B and Shen J: Effects of TLR4 gene silencing on the proliferation and apotosis of hepatocarcinoma HEPG2 cells. Oncol Lett 11: 3054-3060, 2016.
32. Zhang H and Zhang S: The expression of Foxp3 and TLR4 in cervical cancer: Association with immune escape and clinical pathology. Arch Gynecol Obstet 295: 705-712, 2017.
33. Roy A, Srivastava M, Saqib U, Liu D, Faisal SM, Sugathan S, Bishnoi S and Baig MS: Potential therapeutic targets for inflammation in toll-like receptor 4 (TLR4)-mediated signaling pathways. Int Immunopharmacol 40: 79-89, 2016.
34. Zhou J, Deng Y, Li F, Yin C, Shi J and Gong Q: Icariside II attenuates lipopolysaccharide-induced neuroinflammation through inhibiting TLR4/MyD88/NF-κB pathway in rats. Biomed Pharmacother 111: 315-324, 2019.
35. Yin H, Pu N, Chen Q, Zhang J, Zhao G, Xu X, Wang D, Kuang T, Jin D, Lou W and Wu W: Gut-derived lipopolysaccharide remodels tumoral microenvironment and synergizes with PD-L1 checkpoint blockade via TLR4/MyD88/AKT/NF-κB pathway in pancreatic cancer. Cell Death Dis 12: 1033, 2021.
36. Mitra A, Ahuja A, Rahmawati L, Kim HG, Woo BY, Hong YD, Hossain MA, Zhang Z, Kim SY, Lee J, *et al*: Caragana rosea Turcz methanol extract inhibits lipopolysaccharide-induced inflammatory responses by suppressing the TLR4/NF-κB/IRF3 signaling pathways. Molecules 26: 6660, 2021.
37. Chen X, Zhi X, Yin Z, Li X, Qin L, Qiu Z and Su J: 18β-Glycyrrhetinic acid inhibits osteoclastogenesis in vivo and in vitro by blocking RANKL-mediated RANK-TRAF6 interactions and NF-κB and MAPK signaling pathways. Front Pharmacol 9: 647, 2018.
38. Li T, Li X, Zamani A, Wang W, Lee CN, Li M, Luo G, Eiler E, Sun H, Ghosh S, *et al*: c-Rel is a myeloid checkpoint for cancer immunotherapy. Nat Cancer 1: 507-517, 2020.
39. Hunter JE, Leslie J and Perkins ND: c-Rel and its many roles in cancer: An old story with new twists. Br J Cancer 114: 1-6, 2016.
40. Wang S, Liu Z, Wang L and Zhang X: NF-kappaB signaling pathway, inflammation and colorectal cancer. Cell Mol Immunol 6: 327-334, 2009.
41. Xia Y, Shen S and Verma IM: NF-κB, an active player in human cancers. Cancer Immunol Res 2: 823-830, 2014.
42. Taniguchi K and Karin M: NF-κB, inflammation, immunity and cancer: Coming of age. Nat Rev Immunol 18: 309-324, 2018.
43. Yan W, XU F, Liu A, Cai J and Wang S: Effect of Toll like-receptor 4 on proliferation of cervical cancer cells by NF-κB signaling pathway. Chin J Pathophysiol: 301-307, 2015.
44. Limaiem F, Rehman A, Anastasopoulou C and Mazzoni T: Papillary thyroid carcinoma. In: StatPearls [Internet]. Treasure Island (FL): StatPearls Publishing, 2023.
45. National Health Commission of the People's Republic of China Medical Administration and Medical Administration: Thyroid Cancer Diagnosis and Treatment Guidelines (2022 Edition). Chin J Pract Surg 42: 1343-1357+1363, 2022 (In Chinese).